

ROSAT observations of the RSCVn binary σ Geminorum

Z. Yi¹, Ø. Elgarøy¹, O. Engvold¹, and N.J. Westergaard²

¹ Institute of Theoretical Astrophysics, Oslo, Norway

² Danish Space Research Institute, Lyngby, Denmark

Received 22 December 1995 / Accepted 2 March 1996

Abstract. X-ray observations of the RSCVn system σ Geminorum have been undertaken with the ROSAT observatory. Several spectra of very good signal-to-noise ratio were obtained. Spectral fitting using metal abundances amounting to 50% of solar values reveal two temperature components at 2 MK and 12 MK. Previous EXOSAT observations showed another component at 40 MK. Particular interest is focused on the temporal variations of the X-ray emission. It is found that variations occur on time scales ranging from years to hours and minutes.

Key words: stars: coroneae – X-rays: stars – stars σ Gem

1. Introduction

The RS CVn system σ Geminorum (HD62044, HR 2973) is a well-known RS Canum Venaticorum binary system with a period of 19.605 days (Bopp & Dempsey 1989). The visible primary is a red giant of spectral type K1 III. The secondary is not observed directly and does not eclipse the primary. Photometric observations have revealed the existence of large starspots (Hall 1978; Henry *et al.* 1995). The distance is 55.6 pc (Hoffleit & Jaschek, 1982). The Ca II H and K emissions, UV line emission, and X-ray emission of σ Gem show the usual manifestations of high chromospheric and coronal activity. A summary of the characteristics together with added references to the activity of σ Gem may be found in Strassmeier *et al.* (1988, 1993).

σ Gem has previously been observed in X-rays (Ariel V: Pye & McHardy 1983; HEAO 1: Walter *et al.* 1980; Einstein Observatory: Majer *et al.* 1986; EXOSAT: Singh *et al.* 1987; ROSAT: Dempsey *et al.* 1993) and found to be a copious emitter of X rays. The results of the previous observations are summarized in Table 1. The radio emission at 5 GHz appears to be around 0.7 mJy during quiescent periods (Drake *et al.* 1989), but varies considerably.

Previous studies of active binaries may be explained by assuming the presence of a low temperature (a few MK) com-

ponent and a persistent high temperature (> 20 MK) component (Majer *et al.* 1986; Schmitt *et al.* 1990). Two temperatures are also apparent from analyses with continuous temperature distributions which show two more or less pronounced peaks. According to Mewe (1991), this occurs because these stars may have two loop systems. There is a system with many small loops at low temperature, together with fewer, more extended loops at high temperature. The EXOSAT Observations of σ Gem by Singh *et al.* (1987) was in accordance with these findings, showing a component of 8 MK and another of 40 MK.

The present study is based on ROSAT observations of σ Gem. It is of particular interest to explore the temperature structure of the system and the variability of the X-ray emission with time.

2. ROSAT observations

The X-ray emission of σ Gem was recorded with the position sensitive proportional counter (PSPC) onboard ROSAT. The observations were coordinated with IUE observations and optical observations of starspots. The observing sequences were selected so as to be able to detect a possible rotational modulation. The actual observations were performed on April 22 and 27, and October 9, 1992. Some results were presented by Elgarøy *et al.* (1995). A full account of the study is under preparation. The following discussion is restricted to an examination of the X-ray spectra.

From the ROSAT Public Archives it was possible to supplement our data with another PSPC observing sequence of σ Gem, performed between March 31 and April 1, 1991. Four observations with durations between 600 s and 2000 s were made during about 26 hours.

In Table 2 the observations employed in the present investigation are summarized. The orbital phases have been derived from the data given by Bopp & Dempsey (1989).

3. Analysis

Because of the high photon count rate of σ Gem, spectra can be measured for each individual observation listed in Table 2; hence some information on time variations can be derived. It is

Table 1. Summary of results from previous observations

Mission	Date	N_H cm^{-2}	Temperature MK	EM/D ² $10^{50} cm^{-3} pc^{-2}$		Luminosity $10^{31} ergs s^{-1}$	
HEAO 1 ^a	Oct 1977 Apr 1978	(1×10^{19})	(10)			2.1	
Einstein IPC ^b	Apr 1979	$< 2 \times 10^{20}$	14	3.1		1.8	
Einstein IPC ^b	Oct 1979	$< 2 \times 10^{20}$	15	2.7		1.5	
EXOSAT ME ^c	Oct 1984		8 40	2.3 0.8	3.3 1.0		
EXOSAT LE ^c	Oct 1984		5 40	2.3 0.8	3.3 1.0		

^a Walter et al. 1980^b Majer et al. 1986^c Singh et al. 1987**Table 2.** Summary of observations used in the present investigation

No.	Obs. Date	Julian Day	Orbital Phase	Total Counts	Count Rate
1	March 31, 91	2448346.43	0.0967	16227	9.17
2	April 1, 91	2448347.47	0.1497	12672	9.93
3		2448347.47	0.1498	12672	10.31
4		2448347.48	0.1503	17252	9.78
5	April 22, 92	2448734.66	0.8998	12712	8.14
6		2448734.73	0.9034	8571	8.53
7		2448734.80	0.9069	5718	8.70
8		2448734.86	0.9049	6223	8.49
9	April 27, 92	2448739.04	0.1232	15302	8.45
10		2448739.11	0.1268	16376	8.53
11	October 9, 92	2448904.07	0.5411	9529	6.63

Table 3. Summary of spectral fitting.

No.	T_1 MK	ε_1^a $10^{50} cm^{-3} pc^{-2}$	T_2 MK	ε_2^a $10^{50} cm^{-3} pc^{-2}$	L_X^b $10^{31} erg s^{-1}$	χ_{red}^2
1	2.15 (1.91-2.32) ^c	1.08 (0.97-1.19)	11.77 (11.41-12.09)	4.80 (4.57-5.04)	2.46	1.02
2	2.08 (1.65-2.39)	1.13 (0.88-1.35)	11.66 (10.89-12.27)	5.17 (4.65-5.64)	2.65	0.68
3	2.31 (1.93-2.85)	1.01 (0.79-1.22)	12.17 (11.62-12.77)	5.87 (5.39-6.34)	2.80	0.75
4	2.41 (2.23-2.90)	1.10 (0.99-1.22)	12.02 (11.70-12.57)	5.35 (5.10-5.61)	2.67	0.96
5	2.27 (2.04-2.48)	0.92 (0.80-1.03)	11.88 (11.49-12.25)	4.59 (4.34-4.84)	2.29	0.82
6	2.39 (2.17-2.71)	1.24 (1.10-1.39)	11.92 (11.37-12.46)	4.45 (4.12-4.78)	2.39	0.67
7	2.31 (1.97-2.73)	1.08 (0.88-1.25)	11.93 (11.25-12.57)	4.75 (4.31-5.19)	2.42	0.63
8	2.05 (1.68-2.36)	1.02 (0.82-1.20)	11.66 (10.94-12.25)	4.52 (4.08-4.92)	2.33	0.68
9	2.32 (2.14-2.48)	1.06 (0.95-1.17)	11.69 (11.30-12.03)	4.54 (4.31-4.77)	2.37	0.79
10	2.25 (2.08-2.40)	1.14 (1.03-1.24)	11.51 (11.13-11.86)	4.40 (4.17-4.62)	2.37	0.86
11	2.39 (2.20-2.66)	1.07 (0.96-1.18)	11.23 (10.62-11.82)	3.08 (2.85-3.31)	1.82	0.73

^a ε is the specific emission measure, i.e. EM/D^2 with EM in cm^{-3} and D (the distance to the star) in pc.^b $10^{31} erg s^{-1}$ ^c 90% confidence ranges for each fitting parameter.

also possible to divide the data in 402 s bins (402 s is the known wobble period of ROSAT) and look for short time variations.

The spectra were extracted from a circle of 2' centered on the X-ray peak of the PSPC broad-band images. Since the integration time of each spectrum is from 600 s to 1900 s, the spectra comprise at least 5700 counts (see Table 2). As a rule, all bins with a signal-to-noise ratio less than 3 were discarded. Each bin

contains therefore at least 15 photons. The number of degrees of freedom in the resulting spectra is about 150.

The data reduction (i.e. background subtraction) was performed in the IRAF/PROS software package, while the subsequent rebinning of pulse height channels occurred under FTOOLS. The final spectral fitting was carried out in the XSPEC (X-ray Spectral Fitting) package.

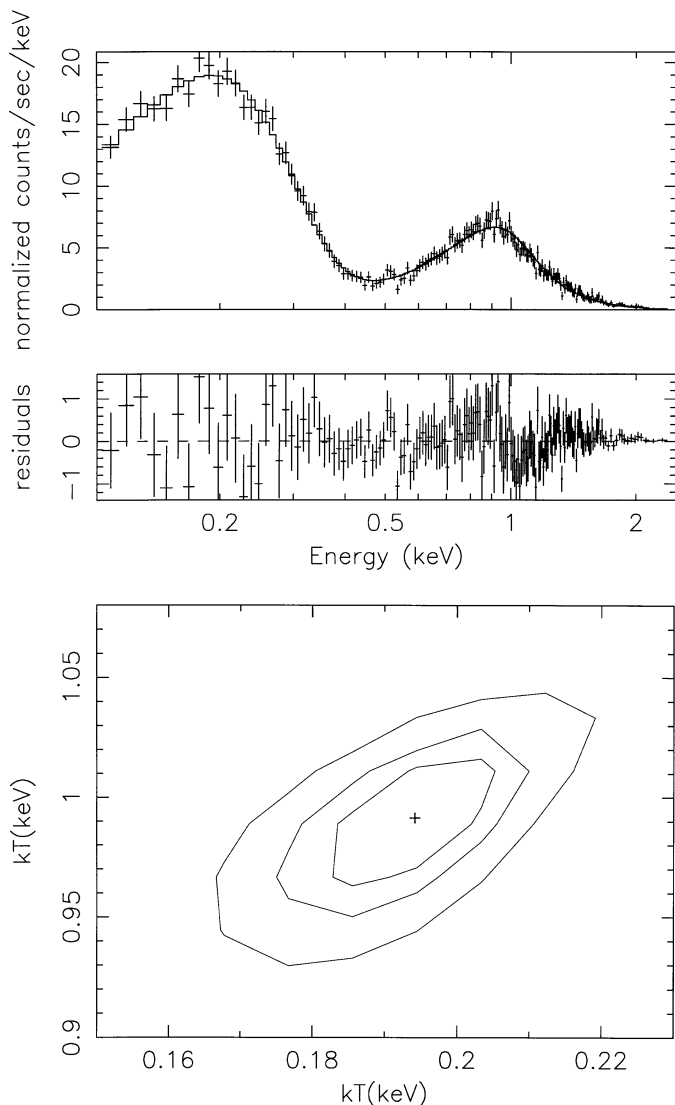


Fig. 1. **a** The pulse height spectrum (no. 10 in Table 2) and the best fitting. The bottom panel in the figure shows the corresponding residuals of the fitting. **b** The confidence contours for the two temperature fit. The contour lines represent confidence level of 99%, 90%, and 68.3%, respectively.

Due to the low spectral resolution of the PSPC, individual spectral lines are invisible. The resulting pulse height spectra can be modeled by a hot, optically thin plasma with line emission from prominent ions, convolved with the PSPC detector response matrix, to estimate source temperatures and emission measures. The Raymond-Smith plasma code (Raymond & Smith 1977) was employed for the spectral fitting. When using this code one should be aware that there may be systematic errors associated with errors in the underlying atomic physics (missing lines, inaccurate oscillator strengths). Furthermore, steady state ionization equilibria are assumed and photoionization is ignored. Therefore, if much of the plasma is in a flaring state, systematic errors imply that temperatures and emission measures may be less accurate than appears from the stated random errors.

There is evidence of reduced metal content in σ Gem. A reduction of 50% as compared to Solar values has been adopted. This is in agreement with the observational results of Randich et al. (1994), regarding photospheric abundances. Coronal and photospheric abundances may be different especially for low first ionization potential elements like Fe (FIP effect). The first ionization potential of Fe is 7.87 eV, and it should have an enhanced abundance in the corona. The FIP effect has been studied in only a few stars and was not detected in Procyon, where coronal abundances were in agreement with their photospheric values (Drake et al., 1995).

All 11 spectra can be well fitted with a two temperature model. Five parameters were involved in the fitting procedure: the interstellar hydrogen column density N_H , two temperatures and their corresponding emission measures. Since σ Gem is rather close, at a distance of 55.6 pc, and the PSPC is insensitive to the expected low value of the interstellar hydrogen column density, N_H was kept fixed at an average value of $2.89 \times 10^{19} \text{ cm}^{-2}$ obtained from the pre-fitting. Thus, the number of parameters to be fitted was reduced to four. Fig. 1 shows one of the PSPC spectra for σ Gem together with the curve which best fitted the data. The results for all observations are summarized in Table 3. Clearly, acceptable fits were derived in all cases ($\chi^2 \leq 1$). One temperature models did not yield satisfactory fits to the PSPC spectra.

X-ray observations of cool stars (RSCVn systems) are usually best explained using two-temperature models when 50% of Solar elemental abundances are assumed. But if the metal content is further reduced, satisfactory model fits can be obtained with one temperature (Kürster & Schmitt 1995). We therefore selected one of our ROSAT observations (no. 10 in Table 2), and tried to fit a one temperature model with reduced metal abundance to the data. Excellent agreement was obtained for $T = 10$ MK when the metallicity was reduced to 0.18 of the Solar value. But such a low metal content is in disagreement with the results of Randich et al. (1994) for σ Gem.

4. Discussion

The ROSAT PSPC spectra of σ Gem show two temperature components, at 2 MK and 12 MK. Previously another component at 40 MK (Singh et al. 1987) was obtained from EXOSAT observations (ROSAT is rather insensitive for gas at this temperature). The corona of σ Gem therefore seems to accommodate plasma at three characteristic temperatures. This situation has a Solar analogy: quiet corona (low temperature), active regions (medium temperature), and regions connected with magnetic field disruptions (highest temperature). This is not to be interpreted so as to imply that there is only coronal plasma at two or three discrete temperatures. The coronal plasma is likely to have a wide range of temperatures.

It is noteworthy that the emission measure for the medium temperature (12 MK) component is 4-5 times larger than that of the lower temperature (2MK) component. Furthermore the emission measure of the 12 MK component is about 3 times larger than that of the 40 MK component (see Tables 1 and 3).

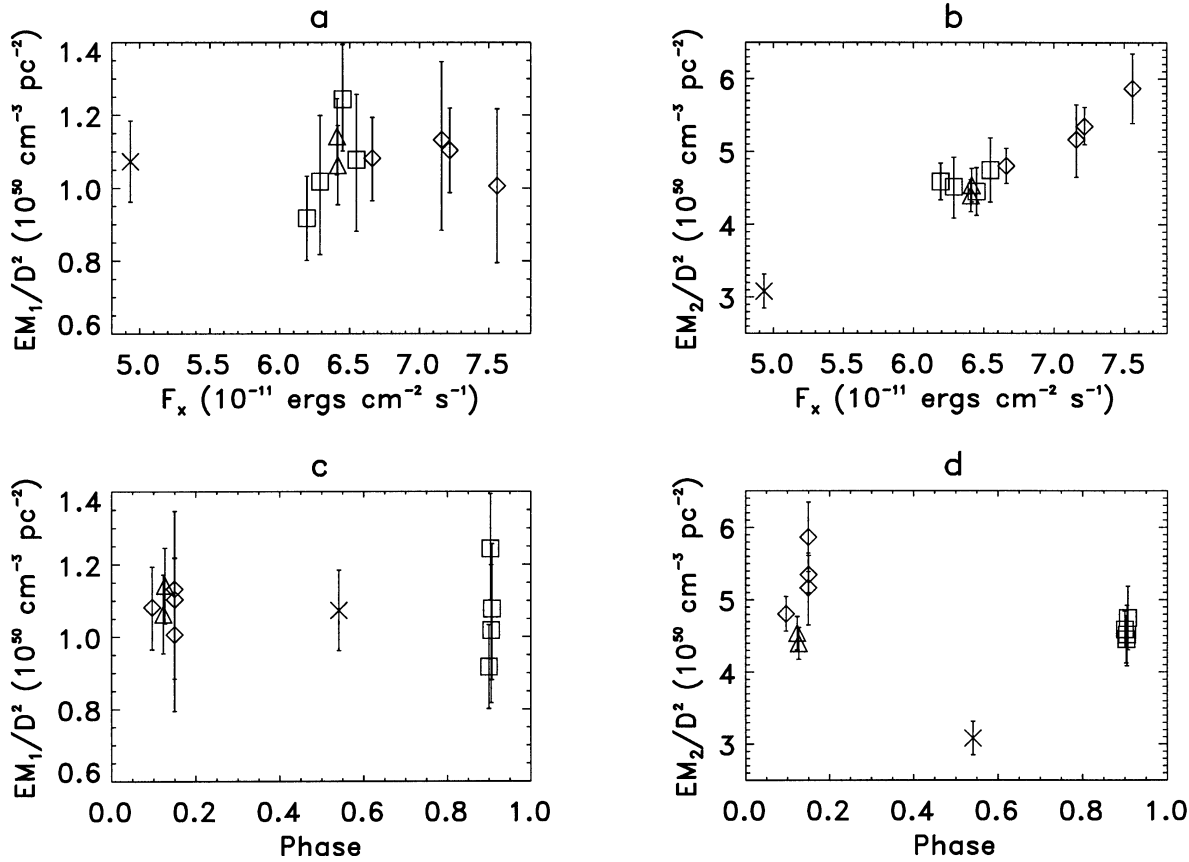


Fig. 2a–d. Emission measures at low temperature **a** and high temperature **b** versus total X-ray fluxes. The symbols diamond, triangle, square, and cross represent, respectively, results for March 30 to April 1 1991, April 22 1992, April 27 1992, and Oct. 9 1992. The lower panels **c** and **d** show the variations of emission measures with the orbital phase. The error bars represent the 90% confidence limits.

This implies that the emission from active regions is very important. The results are in good accordance with the results of Schrijver et al. (1995), who found that their EUVE observations of σ Gem might be explained by a 3–5 MK component, a stronger 15 MK component and a relatively strong component with temperatures exceeding 20–30 MK, when Solar abundance values were assumed. But when the iron abundance was halved, the 20–30 MK component disappeared. Contemporaneous observations with EUVE and ASCA are desirable in order to settle the question of the coronal Fe abundance.

Further evidence in favor of the suggestion that the 12 MK component is associated with emission from active regions comes from the fact that the emission measure of this component shows rapid variations (see Fig. 2d). There is a significant increase of the emission measure of the 12 MK component from March 31 through April 1, whereas changes in 2 MK emission are small. Rapid changes in X-ray emission is likely to occur if the emission is confined to (relatively few) active regions on σ Gem. The quiet (2 MK) component should be rather stable, as is actually found.

The increase in the EM of the 12 MK component leads to an increase in the total X-ray emission, and again suggests that the active regions dominate the X-ray emission on σ Gem. One does not see any strong variations in the temperature (Fig. 3).

The energy relations between the 2 MK, 12 MK, and the 40 MK plasma components may be estimated when the respective emission measures and electron densities are known. One has

$$EM = n_e^2 V \quad \text{and} \quad E = n_e k T V \quad (1)$$

hence

$$E = EM k T / n_e \quad (2)$$

where E is the energy of the gas, n_e is the electron density, k is Boltzmann's constant and T the temperature. Average emission measures for the 2 MK and 12 MK components may be found from Table 3. The emission measure for the 40 MK component is given in Table 1. The following relations are then found:

$$E(2) : E(12) : E(40) = 1 : 23 (n_{e2}/n_{e1}) : 13 (n_{e3}/n_{e1}) \quad (3)$$

where $n_{e1,2,3}$ are the electron densities associated with, respectively, the 2 MK, 12 MK, and the 40 MK components.

The electron density is likely to be higher in the active region corona than in the quiet regions. An important aspect of the above relation is that the two higher temperature components are dominating over the low temperature component which we associate with quiet regions. If the inclination of σ Gem is small

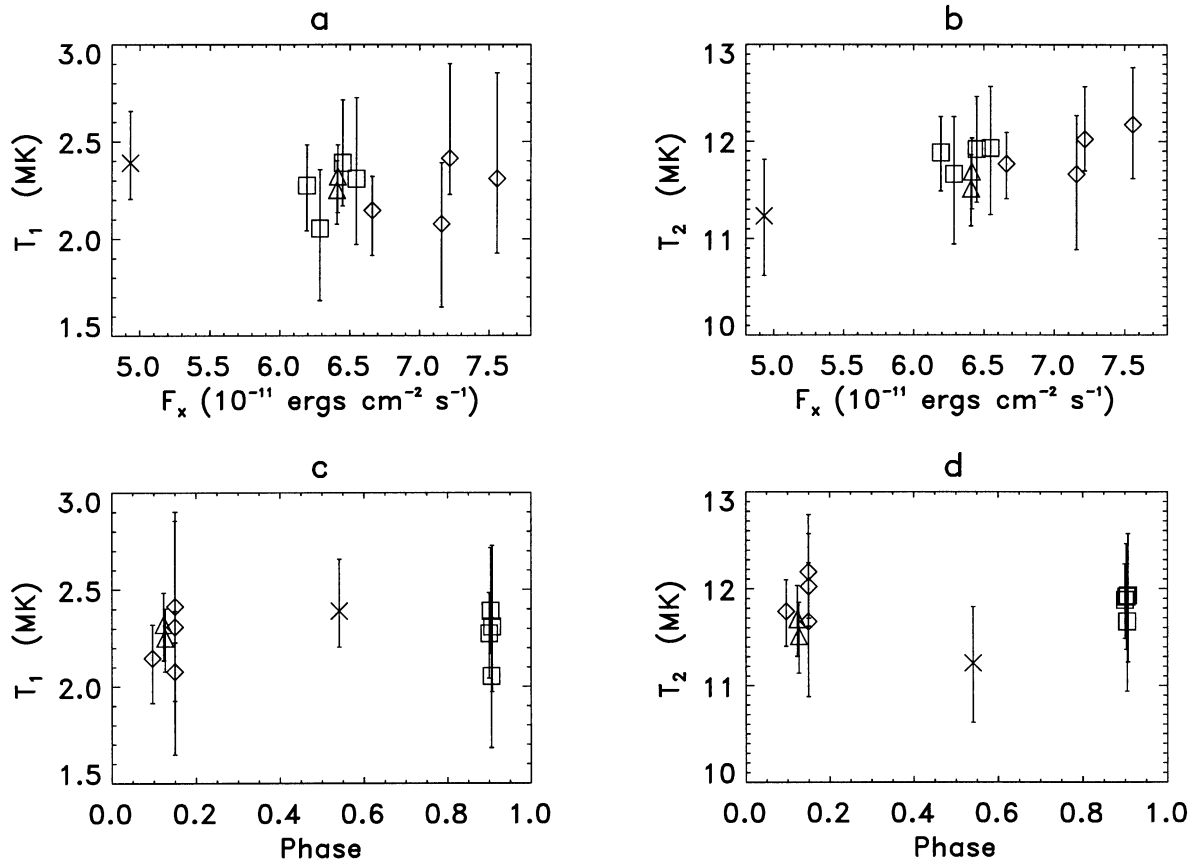


Fig. 3a–d. Best fit to the two temperatures T_1 **a** and T_2 **b** versus total X-ray fluxes. The symbols diamond, triangle, square, and cross represent, respectively, results for March 30 to April 1 1991, April 22 1992, April 27 1992, and Oct. 9 1992. The lower panels **c** and **d** show the variations of temperatures with the orbital phase. The error bars represent the 90% confidence limits.

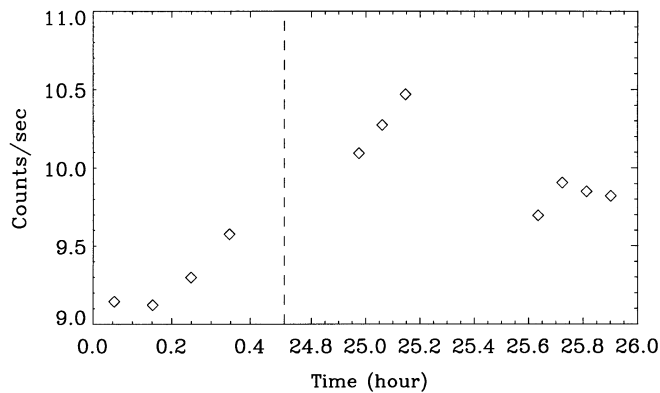


Fig. 4. Time variation of the count rate for the observations from March 31 to April 1, 1991. The telescope wobbling has been removed by rebinning the data in 400 s bins.

(35 degrees according to Dümmler, 1995) and the spotted regions are at high latitudes, the above result appears quite reasonable. The result is in accordance with the results of Schrijver et al. (1995) who found, from EUVE observations of σ Gem, that the emission measure below 2 MK was relatively low.

One may conclude from the above discussion that σ Gem shows a weak plasma component in the one MK range, but the bulk of the plasma is at temperatures in the range between a few MK and 15 MK. There may also be plasma at higher temperatures in the range of some tens of MK. If the latter component is associated with field disruptions, it may be rather variable. More observations to this point are highly desirable.

The UV, X-ray and radio emission of σ Gem is quite variable. A long term activity cycle of 8.5 years has been detected by Henry et al. (1995). From Table 2 one notes a systematic difference between the count rates in the 1991 and 1992 observations. This may be an outcome of the activity cycle, but far more observations are needed in order to reach a conclusion.

It was found by Elgarøy et al. (1995) that a possible rotational modulation was masked by stronger short time fluctuations in the UV range. Our ROSAT observations show that short time fluctuations also occur in the X-ray range. From Table 2 and 3 together with Fig. 2 it may be concluded that variations in the emission occur on a time scale corresponding to the time between subsequent observing sequences, i.e. about 1.5 hours.

In order to search for variations on the shortest possible time scale, we selected three of the longest observations and binned the data in 402 s bins (according to the wobbling period of ROSAT). Fig. 4 shows that there are variations on a time scale

of the order of some minutes. Taking into account our whole set of X-ray observations one may conclude that there is good evidence for intensity variations on time scales ranging from years to minutes. Existing observations are far too scanty to give a good insight into the time variation of the chromospheric and coronal emissions of σ Gem and their underlying physical causes, but present evidence has at least shown that further observations may give interesting results.

Radio observations of several RSCVn systems (Lefèvre et al. 1994) with high time resolution showed that the emission was time variable both during flares as well as during a significant fraction of the “quiescent” phases, on time scales ranging from minutes to some hours. It was concluded that low level flaring must be a permanent feature of these stellar atmospheres. It is in good accordance with our findings concerning UV and X-ray emission from σ Gem.

5. Conclusions

σ Gem accommodates gas at a wide range of temperatures. The cooler plasma may be associated with quiet regions and is relatively stable. A hotter component, in the range of about 10 MK, originates from active regions and is rather variable. A very hot component may be present, probably associated with magnetic field disruptions.

Using all available ROSAT observations of σ Gem one has obtained some information on possible temporal variations in the X-ray emission. The component associated with active regions shows variations on the scale of one year, which may be linked with long term (cyclic) variations of activity. Rotational modulation (19.6 days) has not been detected, but more observations are needed to establish the possible absence of such variations. For the first time sufficient observations have been obtained to demonstrate variations on time scales ranging from hours to minutes. Such variations are to be expected when the highly active character of σ Gem is taken into account, and is in accordance with results from radio observations of RSCVn systems.

The observations give some support to a model in which quiet region plasma (loops) have temperature around 2 MK. In active regions magnetic field reconnection occurs at large heights and high temperature (40 MK) accelerating oppositely directed particle streams (jets). The downward directed particles impinge on underlying closed loops, create shocks and heat the loops to temperatures around some 10 MK. The structure of the active region corona of σ Gem may have some properties in common with the model proposed by Shibata et al. (1995) in order to explain compact-loop solar flares.

Acknowledgements. The authors would like to express their thanks to the referee, J. Linsky, for valuable comments.

References

- Bopp, B.W., Dempsey, R.C.: 1989, PASP 101, 516
 Dempsey R. C., Linsky, J. L., Schmitt, J.H.M.M & Fleming, T. A.: 1993, ApJ 413, 333
 Drake, S. A., Simon, T., & Linsky, J. L.: 1989, ApJS 71, 905
 Drake, S.A., Laming, J.M., Widing, K.G.: 1995, ApJ 443, 393
 Dümmler, R.: 1995, Poster paper at IAU Symp. 176 “*Stellar Surface Structure*”, Vienna, 1995, ed. Strassmeier K. G.
 Elgarøy, Ø, Engvold, O., Jorås, P.: 1995, Strassmeier K. G. (ed), Poster Proc. IAU Symp. 176, “*Stellar Surface Structure*”, Vienna, p. 165
 Hall, D. S.: 1978, AJ, 83, 1469.
 Henry, G. W., Eaton, J. A., Hamer, J.: 1995, ApJ S 97, 513
 Hoffleit, D., Jaschek, C.: 1982, in “*The Bright Star Catalogue*”, Yale University Observatory, New Haven.
 Küster, M., Schmitt, J.H.H.M.: 1995, Strassmeier K. G. (ed), Poster Proc. IAU Symp. 176, “*Stellar Surface Structure*”, Vienna, p. 200
 Lefèvre, E., Klein, K.-L., Lestrade, J.-F.: 1994, A&A 283, 483
 Majer, P., Schmitt, J.H.M.M., Golub, L., Hamden, Jr. F. R., Rosner, R.: 1986, ApJ 300, 360
 Mewe, R.: 1991, Adv. Space Res. 11, 127
 Pye, J. P. & McHardy, I. M.: 1983, MNRAS 205, 875
 Randich, S., Giampapa, M. S., Pallavicini, R.: 1994, A&A, 283, 893
 Raymond, J. C., Smith, B. W.: 1977, ApJS 35, 419
 Schmitt, J.H.M.M., Collura, A., Sciortino, S., Vaiana, G. S., Hamden, Jr. F. R. & Rosner, R.: 1990, ApJ 365, 704
 Schrijver, C. J., Mewe, R., van den Oord, G.H.J, Kaastra, J. S.: 1995, A&A 302, 438
 Shibata, K., Masuda, S., Shimojo, M. et al.: 1995, ApJ 451, L83
 Singh, K. P., Slijkhuis, S., Westergaard, N. J., Schnopper, H. W., Elgarøy, Ø., Engvold, O. & Jorås, P.: 1987, MNRAS 224, 481
 Strassmeier, K. G., Hall, D. S., Zeilik, M. et al.: 1988, A&AS, 72, 291
 Strassmeier, K. G., Hall, D. S., Fekel, F.C., & Scheck, M.: 1993, A&AS, 72, 291
 Walter, F. M., Cash, W., Charles, P. A. Bowyer, C. S.: 1980, ApJ. 236, 212